Research Article

Journal of Environmental Nanotechnology

Effect of Silicon Dioxide Nanofiller on Mechanical and Sliding Wear Properties of *Agave fourcroydes* Fibre-reinforced Epoxy Composites

P. Satishkumar[1*], Rajasekaran Saminathan[2], Divya Raju[3], K. Maheswari[4], S. Mohamed Nasrulla[5] and R. Sathishkumar[6]

[1]Department of Mechanical Engineering, Rathinam Technical Campus, Coimbatore, TN, India
[2]Mechanical Engineering Department, College of Engineering and Computer Science, Jazan University, Saudi Arabia
[3]Department of Nursing, College of Applied Health Sciences and Nursing, Jazan university, Saudi Arabia
[4]Department of Computer Science and Engineering, CMR Technical Campus, Hyderabad, TG, India
[5]Department of Mechanical Engineering, PSNA College of Engineering & Technology, Dindigul, TN, India
[6]Department of Science and Humanities, Rathinam Technical Campus, Coimbatore, TN, India
Received: 06.06.2025 Accepted: 27.08.2025 Published: 30.09.2025
*sp.sathishkumar10@gmail.com

ABSTRACT

The mechanical properties and sliding wear behavior of epoxy composites reinforced with *Agave fourcroydes* (AF) fibers were studied to investigate the synergistic effect of hybridizing silicon dioxide (SiO_2) filler. The experimental results reveal that the combination with 10 wt % AF/5 wt % SiO_2 showed better mechanical results (tensile strength 55.99 MPa, flexural strength 31.67 MPa and impact energy of 4.225 J). In contrast, higher hardness (45.87 HV) was achieved at 10 wt % *AF*/7 wt % SiO_2 composites. Deterioration of mechanical properties was noticed at higher silicon dioxide (7 wt %) loading due to uneven distribution and particle agglomeration in AF-epoxy composites. The control parameters were sliding velocity (2 m/s - 5 m/s), SiO_2 content (0 wt % - 7 wt %), and normal load (20 N - 35 N). The optimization of the sliding wear rate was analyzed by Taguchi approach, followed by an analysis of variance used for evaluating the significance of control parameters. The results showed a combination with SiO_2 content of 7 wt % (60.7 %) > normal load of 35 N (46.9 %), > sliding velocity of 5 ms^{-1} (0.4 %) exhibited an optimum value of specific wear rate.

Keywords: Wear rate; *Agave fourcroydes*; Flexural strength; Optimization; Mechanical properties.

1. INTRODUCTION

The biodegradability, ecological responsibility, and usability of natural fibers have gained attention of academic and industrial researchers. Compared to natural fibers like jute, sisal, and flax, *Agave fourcroydes* exhibits higher cellulose content, comparable tensile strength (up to 30–35 GPa modulus), and better thermal resistance (up to 350 °C). These properties make it more suitable for applications in structural, automotive, and thermal insulation composites where enhanced mechanical stability and sustainability are required. Lakshmaiya *et al*. (2025) employed Taguchi L27 orthogonal array and ANN modeling to optimize the mechanical behavior of pineapple fiber/nano-SiO_2 reinforced composites. The best performance was observed for 20 % fiber (10 mm length), 5 % nano-SiO_2, and six-hour NaOH treatment, improving tensile, flexural, and impact strength. ANOVA indicated that NaOH treatment was the most influential factor (45 %), with ANN predictions matched the experimental values within 4 %.

Bamboo fiber/nano-SiO_2 composites were fabricated and optimized using response surface methodology with a central composite design. The 32H and 32G composite variants exhibited peak tensile and flexural strength, respectively, with optimal reinforcement at 2 wt % nano-SiO_2 and two bamboo fiber layers. A quadratic regression model with high R^2 values confirmed the mechanical robustness and application potential in structural and automotive sectors (Kumar *et al*. 2024). Devendrappa *et al*. (2022) compared sisal-glass hybrid epoxy composites filled with graphite, focusing on mechanical and wear behavior. Graphite fillers enhanced flexural modulus by 35.2 % and improved impact and hardness values. Natural fibers showed higher wear than synthetics. ANOVA revealed that reinforcement type contributed 57.99 % to wear rate variation, supporting natural-synthetic hybrids for eco-conscious structural uses.

Polylactic acid (PLA)-based hybridized composites with sugarcane bagasse and chicken feather fibers were fabricated using compression molding and evaluated for wear performance. Tribological testing identified optimal combinations for reduced wear using Taguchi L18 orthogonal array. The study promotes eco-friendly biofiber, PLA hybrids for tribological

applications using low-cost, locally available materials (Mathur *et al*. 2024). Composites combining human hair, Luffa fibers, and incense stick ash (ISA) were synthesized and tested for mechanical and wear behavior. The composite with 10 wt % ISA showed maximum mechanical strength, and 15 wt % ISA yielded the highest energy dissipation. Wear was optimized using gray relational analysis and Whale Optimization Algorithm, with SEM confirming the wear mechanisms (Rout *et al*. 2025). Flax fiber-reinforced epoxy composites with TiO_2 fillers (0–8 wt%) were fabricated and tested for abrasive wear using Taguchi DOE and ANOVA. Grit size was the most significant factor (43.78 %) affecting specific wear rate (SWR), followed by load and TiO_2 content. The optimized composition enhanced wear resistance, validating the use of TiO_2 in sustainable natural fiber-reinforced composites (NFRCs) (Prabhu *et al*. 2024).

Hybrid epoxy composites were developed using bidirectional bamboo fiber and nano-silica (0–4 wt %) by the hand lay-up technique. Hybrid composite with 4 wt % showed highest heat resistance, but mechanical properties declined beyond 3 wt % nano-SiO_2 due to particle agglomeration. The FESEM, XRD, FTIR, and water absorption studies confirmed optimal reinforcement balance around 2–3 wt % SiO_2.

Natural fiber composites reinforced with alkali-treated *Phaseolus vulgaris* fiber (PVF) and fly ash/nano-SiO_2 in a polyester matrix were studied. Mechanical, thermal, and dielectric properties peaked at 6 % PVF with 1 % $nSiO_2$, while higher PVF caused property degradation. The composite demonstrated optimal performance at 6 % PVF for structural insulation applications (Gurukarthik *et al*. 2021). Jute fiber–reinforced vinyl ester composites with and without SiO_2 filler were compared for mechanical properties. SiO_2 inclusion enhanced tensile strength by 50 % and other properties by 5–10 % due to improved fiber-filler interfacial bonding. The SEM analysis validated the mechanical reinforcement effect of nano- SiO_2 in NFRCs (Padma *et al*. 2022). A hybrid composite with 25 % ramie, 15 % kenaf, and 2 % TiO_2 was fabricated and tested for mechanical performance. Results showed tensile strength of 66.14 MPa, flexural strength of 86.46 MPa, and high impact resistance, combining strength and eco-friendliness. The TiO_2 addition enhanced overall performance, making the material suitable for high-load and sustainable applications (Mary *et al*. 2024).

Banana-papaya fiber epoxy composites with tri-layer stacking (PBP and BPB) were enhanced with 2–3 wt % nano-SiO_2. The PBP/2 % SiO_2 composite achieved the highest mechanical strength (tensile: 83 MPa, flexural: 104 MPa), excellent thermal stability, and low water absorption. These hybrids offer promising sustainability and durability for automotive and marine applications (Kedarnath *et al*. 2025). Two eco-friendly insulation prototypes were developed using *Agave fourcroydes* (henequen) and *Washingtonia filifera* (palm) fibers, pulped by alkali treatment, and optimized using Taguchi design. Henequen-based material achieved thermal conduction of 0.036 WmK^{-1} and palm-based 0.0409 WmK^{-1}, that are comparable to commercial insulators like expanded polystyrene. These findings promote their application in sustainable building materials to reduce energy consumption (Rosas *et al*. 2024). A recent study linked CesA gene expression to fiber quality in *Agave fourcroydes* by evaluating CesA3, CesA4, and CesA5 gene activity and fiber composition in plants of varying heights. High cellulose content (48 %) and longer leaves correlated with high CesA3 and CesA4 expression and lower CesA5 expression. These genetic markers aid in the early selection of high-cellulose plants for fiber improvement and crop breeding (Salinas *et al*. 2023). Henequen fiber-reinforced polypropylene (PP) composites were evaluated using micromechanical modeling and tensile tests, showing Young's modulus increases up to 327 % with 50 wt % fiber. The fiber's intrinsic modulus ranged from 30.5–34.6 GPa, confirming its stiffness comparable to glass fiber in PP matrices (Serra *et al*. 2021).

Injection-molded PP composites with henequen fiber were analyzed with and without coupling agents. Aspect ratio and interfacial quality strongly influenced reinforcement efficiency and composite mechanical performance (Espinach *et al*. 2022). Raw henequen fibers were characterized for composite applications, showing 42.4 % crystallinity (XRD), TS of 21.12 MPa, and modulus of 8.3 GPa. Antibacterial activity, UV resistance, and thermal firmness upto 350 °C demonstrate multifunctional potential for sustainable composites (Raja *et al*. 2025). NaOH-treated henequen fibers reinforced phenolic composites by hot pressing showed improved tensile strength (at 50 % fiber) but slightly reduced flexural strength. Treated composites were found to be suitable for construction elements like artificial roofing and wall panels (Seeniappan *et al*. 2024).

Polyamide 6 (PA6) composites reinforced with raw and alkali-treated chopped henequen fibers were processed through extrusion and injection molding. Side feeding and NaOH treatment enhanced mechanical properties compared to hopper-fed and untreated fibers. This approach demonstrates improved mechanical integration in engineering thermoplastics (Kim *et al*. 2022). Gavidia *et al*. (2024) evaluated epoxy composites strengthened with coconut, jute, and henequen fibers for aerospace applications. Tensile test, flexural test, and impact tests were performed at 45° and 90°, followed by finite element simulations. The selected composite ensured high structural integrity, achieving safety factors of 10 (axial) and 15 (lateral) in a 3000 m apogee rocket design.

Bagasse-henequen fiber-reinforced epoxy/vinyl ester composites were prepared with untreated and

NaOH-treated fibers (12 and 24 h). The 25 wt % fiber composites with 24 h alkali treatment exhibited the best tensile, flexural, and compressive properties. Treatment duration significantly influenced mechanical performance, validating its optimization for biofiber composites (Venkatesha *et al*. 2021). Sisal fibers embedded in a phenol-formaldehyde matrix with nano-SiO_2 exhibited significantly improved friction and wear performance. Enhanced fiber–matrix bonding and heat resistance made these eco-friendly composites viable alternatives to traditional brake-pad asbestos (Zeng *et al*. 2014). Jute fabric composites incorporating 2–5 wt% nano-SiO_2 showed substantial reductions in wear rate and coefficient of friction under various loads and sliding speeds, demonstrating the filler's effectiveness in improving tribological performance (Erkliğ *et al*. 2022).

Henequen flour (1–5 wt %) reinforced PLA composites were 3D printed and evaluated under tension. At 1 wt % loading, NFRCs showed improved tensile properties compared to neat PLA, while higher contents led to agglomeration and reduced performance. Raster angle and maleic anhydride addition also influenced mechanical behavior, suggesting potential in low-load applications (Agaliotis *et al*. 2022). High density polyethylene composites reinforced with surface-modified henequen fibers were tested for tensile properties and damage evolution. Chemically treated fibers showed a 37 % improvement in maximum load and enhanced interface bonding (Anaya *et al*. 2023). Machine learning and multi-objective optimization (ARAS + GA) were used to enhance the performance of bamboo and madar fiber (BMF)/Nano SiO_2-strength composites for lightweight, low-emission automobile applications. The optimal parameters identified were 10 % Nano SiO_2, 35 % BMF, 24 mm fiber length, and 9 % NaOH treatment. Regression models achieved R^2 |>| 80 %, confirming strong predictive capability for composite performance optimization (Gupta *et al*. 2024). Environment-friendly hybrid composites were fabricated using abaca (76 %) and areca (20 %) fibers with 4% nano SiO_2 in an epoxy matrix, showing superior tensile, flexural, and impact strengths. Nano-silica enhanced interfacial bonding and matrix reinforcement, while hybridization balanced mechanical performance and sustainability. The SEM analysis revealed improved bonding and reduced delamination in the optimized composition (Harak *et al*. 2024).

The primary goal of this article is to examine the mechanical and sliding wear properties of SiO_2 nano-fillers-based AF-epoxy hybrid composites. The sample was prepared by hand layup technique with a varying proportion of nano-filler materials from 0 wt % to 7 wt % at fixed AF fibers (10 wt %). The ranking of selected factors (sliding velocity, silicon dioxide, and normal load) on the sliding wear behavior of the fabricated composites was determined by using an orthogonal array (L16) by Taguchi and an ANOVA. Taguchi method was employed for its efficiency in minimizing the number of experimental trials while systematically analyzing multiple parameters influencing wear performance. ANOVA was used to statistically quantify the contribution of each factor, ensuring the reliability and significance of the observed trends. Together, these methods provide a robust framework for optimizing mechanical and tribological properties in composite materials.

2. EXPERIMENTAL METHODOLOGY

2.1 Reinforcement and Matrix Constituent

Fiber from *Agave fourcroydes* belonging to the Asparagaceae family was collected from Coimbatore, India, and bi-directional mats were prepared with a weight area of 232 gm^2. In this research, silicon dioxide reinforcement was used to hybridize *Agave fourcroydes*. The density and purity of silicon dioxide nanofiller are 3.8 g/cm^3 and 99.9 %, respectively. The silicon dioxide was purchased from Matrics Enterprises, Nagercoil, Tamil Nadu, India. The epoxy resin (grade LY556; density is 1.2 g/cm^3), along with a compatible hardener (HY951), was purchased from Kovai Seenu Enterprises, Coimbatore, Tamil Nadu, India.

2.2 Preparation of Composites

Hand layup technique was employed to produce composite samples in this investigation. The composites were prepared using the following steps (Fig. 1): Mold preparation, reinforcing agent placement, Resin application, Layering, and Curing. Epoxy matrix (LY556), AF fiber, and silicon dioxide nano-fillers were used for the preparation of the composite. Composites were prepared with fixed AF fibre loading 10 wt % inside a wooden mold. The dimensions of a wooden mold, 200 mm × 200 mm × 6 mm, were manually constructed. Composites were fabricated for fixed AF fibre with the addition of varying ranges (0 wt % to 7 wt %) of silicon dioxide nano-filler to improve the mechanical and sliding wear behavior. Then, a 10:1 (standard mixing ratio) ratio of commercial epoxy (LY556) and hardener (HY951) was taken in a beaker and mixed adequately with a hand stirrer. The mold's surface was coated with wax, a mold-removing agent, to facilitate the removal of the fabricated composites. The mold was carefully filled with the epoxy-hardener mixture, and the AF mats were subsequently applied accordingly. After the settlement of the AF mat into the mold, the next mix (epoxy and hardener) was layered. Silicon dioxide-*Agave fourcroydes* hybrid composites were prepared by the incorporation of SiO_2 nanofiller in the mixture of epoxy and hardener. The SiO_2 filler percentages of 0 %, 3 %, 5 %, and 7 % (Table 1) were selected to systematically observe the progressive effect of increasing filler content on the composite's mechanical and wear behavior. A

lower range (3 % and 5 %) was chosen to explore potential reinforcement benefits, while 7% was included to assess the effects of higher filler loading, such as possible agglomeration or reduced dispersion. This range enables identification of the optimal balance between filler content and composite performance. In contrast, the remaining process of composite fabrication is the same as discussed above. Afterward, the casting of each prepared composite was cured at a 10 kg load for 24 hours at normal room temperature. The polymer composites of various compositions were fabricated using a hand layup process (Narayanan *et al*. 2024).

Table 1. Experimental combination of the prepared composites

Designations	AF (wt %)	SiO_2 (wt %)	Epoxy (wt %)
S1	10	0	90
S2	10	3	87
S3	10	5	85
S4	10	7	83

The wear rate (WR) of fabricated composites was calculated as per American standards for testing material (ASTM) standards. Tensile strength (ASTM: D3039) was determined using a universal testing machine (UTM) at a crosshead speed of 2 mm/min and dimensions of 125×12.7×3 mm^3. A flexural test (ASTM: D790-07) was conducted using a UTM with a span-to-thickness ratio of 16:1 and dimensions of 125×12.7×3 mm^3. Vickers's hardness (ASTM: E92 and dimensions 25×25 mm^2) test rig was used for the hardness measurement of composites with an apical angle-6° and the applied load was 5 kg for 15 seconds of dwell time. The impact energy was evaluated by using the Charpy test (ASTM: E23 and 55 × 10 × 10 mm^3) with a 2 mm deep notch at an angle of 45°. Moreover, the specific WR (ASTM: G99 and the dimension of 35×8 mm^2) was determined by using a pin-on-disc (POD) test rig where the steel disc hardness was 74 HRC. During the POD experiment, the pin (sample) was fixed within the specimen holder, and the 74 HRC steel disc rotated at a desirable speed. Preliminarily, the sample was pressurized onto the rotating steel disc with the decided load and time. After completion of the specified time, the samples were taken out and weighed on a digital precision weighing machine. Material removal was evaluated by the variation among the starting mass and ending mass of samples, and the specific wear rate (SWR) was considered by Equation (1). Here, sliding velocity (m/s), SiO_2 content (wt %), and normal load were the significant control factors for the action of SWR on composites (Jagadeesh *et al*. 2024).

$$SWR = \frac{m_i - m_f}{\rho l f_n} \quad \ldots (1)$$

$SWR, m_i, m_f, l, \rho,$ and n represent SWR (mm^3/Nm), initial mass (g), final mass (g), sliding distance (m), density, and normal load (N).

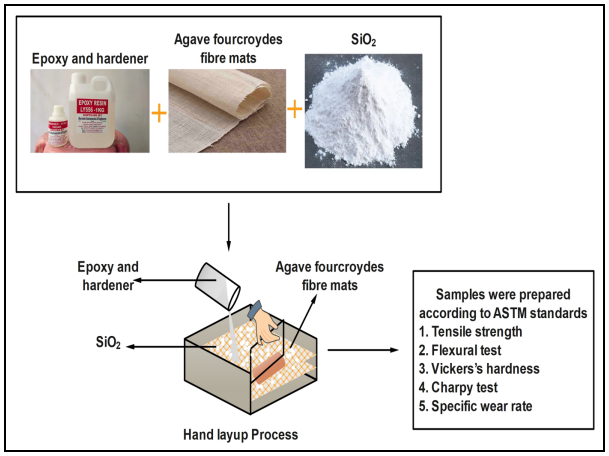


Fig. 1: Experimental procedure for composite material fabrication

2.3. Taguchi Analysis

The Taguchi approach enables a structured analysis of the experimental data, facilitating the identification of optimal factor combinations for enhanced sliding wear performance. Deciding the control factors for the design of the experiment (DOE) was a crucial phase. In this investigation, the control parameters and their levels are selected as follows: sliding velocity (2 m/s, 3 m/s, 4 m/s, and 5 m/s); SiO_2 content (0 wt %, 3 wt %, 5 wt % and 7 wt %); and normal load (20 N, 25 N, 30 N, and 35 N) (Sarkar *et al*. 2023). The optimal combination of control parameters for low wear rate was evaluated using an orthogonal array L_16 that was built using the Taguchi method. It implies that there are 16 different combinations of sliding velocity, SiO_2 content, and normal load systematically arranged for experimentation. However, the actual number of experiments for a conventional complete factorial design is 256 (i.e., 44) to study four factors at four levels, and hence the Taguchi method is reduced to 16 experiments. Further, the output result (SWR) was converted into a signal-to-noise (SN) ratio.

The three distinct kinds of signal-to-noise ratios are as follows: Smaller the better, larger the better, and nominal the better, respectively. This study primarily aims to examine the sliding WR of composites. As displayed in Fig. 3, the experimental design method was based on the lower value of this feature, which was calculated using Equation 2 (Albert *et al*. 2023).

$$S/N \text{ ratio } = -10 \times \log\left(\frac{1}{p}\right)(\sum \delta^2) \quad \ldots (2)$$

Moreover, the percentage of contribution of each selected parameter was done by ANOVA (analysis of variance), and the overall ratio mean was computed as Equation 3.

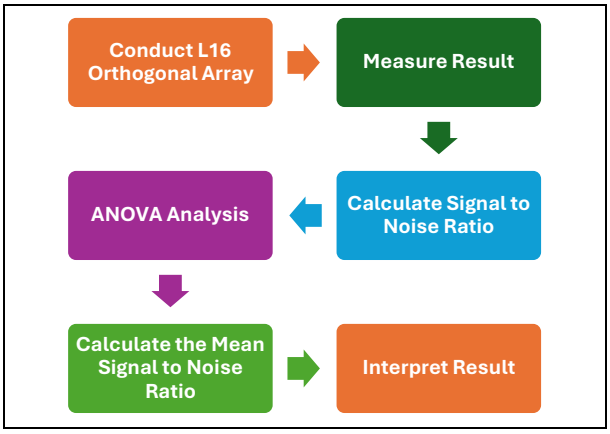


Fig. 2: Systematic experimental framework

$$\overline{S/N} \text{ ratio } = 1/16 \sum_{n=1}^{16} S/N \text{ ratio} \quad \ldots (3)$$

After that, the sum of squares due to variation in ratio was obtained by Equation 4.

$$\sigma = \sum_{n=1}^{16} \left((S/N \text{ ratio })_n - \overline{S/N} \text{ ratio} \right)^2 \quad \ldots (4)$$

For the nth control parameter, the sum of squares due to variation in ratio was evaluated by using Equation 5.

$$\eta_n = \sum_{m=1}^{4} \left((S/N \text{ ratio })_{mn} - \overline{S/N} \text{ ratio} \right)^2 \quad \ldots (5)$$

Finally, the contribution of each parameter is calculated by Equation 6.

$$\text{Percentage of contribution} = \left(\frac{nn}{\sigma} \right) \times 100 \quad \ldots (6)$$

3. RESULTS AND DISCUSSION

3.1. Results on Mechanical Test

Finally, the contribution of each parameter was calculated by Equation 6. As shown in Fig. 3, 4, and 6, the TS, FS, hardness, and impact energy of the manufactured composites were assessed about the silicon dioxide concentration. It is evident that when silicon dioxide content was incorporated into the AF-epoxy composite, it yielded a gradual increase in mechanical properties up to 5 wt % filler loading, due to better dispersion of nanoparticles within the epoxy matrix, which enhanced stress transfer and reduced microvoids. At this level, an optimal balance between filler reinforcement and matrix integrity was achieved. The highest value of tensile strength was achieved for the S3 composite, i.e. 55.99 MPa. However, at 7 wt %, performance declined, mainly due to nanoparticle agglomeration. These agglomerates act as stress concentrators, weaken the fiber–matrix interface, and introduce defects, leading to reduced tensile and flexural strength. Excess filler also stiffens the matrix, making it more brittle and prone to crack initiation. After that, deterioration in tensile strength (8.43 %) has been seen for composites, which is 51.27 MPa. Thus, 5 wt % SiO_2 was found to be the optimal loading for improved mechanical behavior.

Similarly, epoxy composites reinforced with *Terminalia arjuna* fiber (up to 30 wt %) and nano- SiO_2 (2 wt %) showed excellent mechanical and water resistance properties. The composite achieved 74 MPa tensile strength and 6.6 kJ/m^2 impact resistance with only 18.4 % water absorption (Arumugam *et al.* 2024). This phenomenon is perceived to be due to the high dispersion of silicon dioxide filler, which increases the interaction among the AF fibre, epoxy, and the dispersed particles, leading to improved TS. Further, the TS decreases for S4 composites due to increased void fractions and brittleness of the SiO_2-filled AF-epoxy composites.

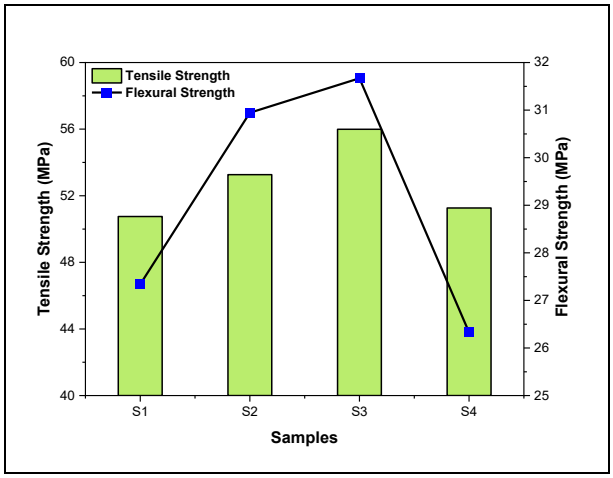


Fig. 3: Evaluation of tensile strength and flexural strength with respect to varying SiO_2 content of fabricated composites

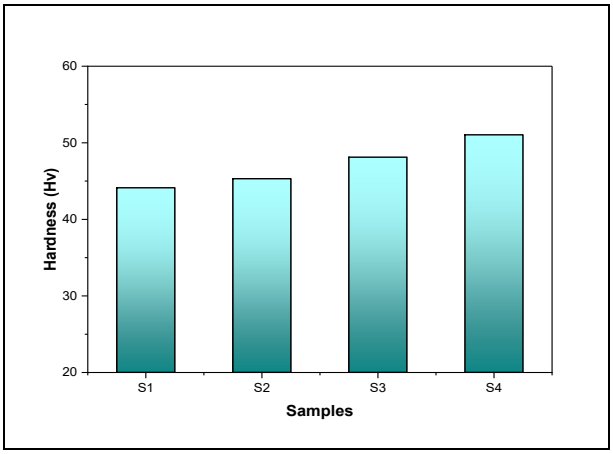


Fig. 4: Evaluation of hardness with respect to varying SiO_2 content of fabricated composites

Epoxy composites reinforced with *Cissus quadrangularis* stem fiber and nano-SiO_2 (0–2 wt %) achieved a TS of 118.1 MPa and FS of 132.6 MPa at 2 wt % filler. Impact strength peaked at 1.5 wt % filler, and thermal, acoustic, and water absorption properties were improved. The SEM analysis confirmed better fracture resistance and filler dispersion (Iyyadurai *et al*. 2023). In the present study, the flexural strength of the composites varies from 27.34 MPa to 31.67 MPa for zero wt % to 5 wt % of silicon dioxide filler (Fig. 4). However, the FS increased with the addition of the SiO_2 content. 5 wt % filler (S3) composites have attained higher flexural strength, which is 9.35 % more than 0 wt % nano-fillers (S1) composites. Further, the addition of silicon dioxide (7 wt %) nano-fillers in AF-epoxy composites slightly deteriorated the FS of the composites (26.33 MPa). The increment in flexural strength caused by the better interfacial adhesion between the constituents of the composites and voids in the composites will be occupied by the filler. The SiO_2-filled composite showed the best mechanical performance: tensile strength (88 MPa), impact strength (9.5 kJ/m^2), and hardness (77 Shore-D), while the natural composites made with 70:30 epoxy/peepal fiber were reinforced with 2 wt % SiO_2, SiC, and hybrid fillers (Vignesh *et al*. 2024).

Fig. 5(a) shows visible fiber pull-out and poor interfacial bonding, indicating weak load transfer between fiber and matrix. Fig. 5(b), better fiber–matrix adhesion, reduced pull-out, and uniform filler dispersion are observed, contributing to higher tensile and flexural strength. Fig. 5(c) reveals regions of filler agglomeration and voids, which act as stress concentrators and reduce mechanical performance at higher filler loadings. Nevertheless, there are still some visible voids. The existence of fiber/matrix bonding and uniform dispersion of silicon dioxide fillers in the epoxy was seen in the SEM micrograph. Therefore, the combination of agglomeration and fibre pull-out traces of AF fibres in the epoxy has been significantly reduced due to the better dispersion of silicon dioxide fillers in the matrix. Further, silicon dioxide filler was increased from 5 wt % to 7 wt %. Therefore, some agglomerations were detected in the micrograph, and deterioration of tensile strength was observed (Fig. 5c).

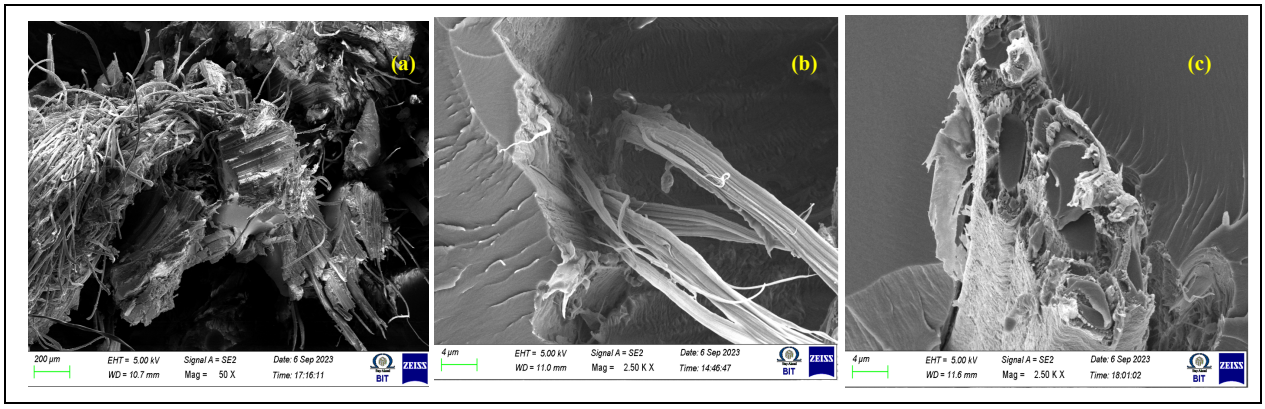


Fig. 5: SEM images of tensile fractured samples of (a) S_2 (3 % SiO_2), (b) S_3 (5 % SiO_2) and (c) S_4 (7 % SiO_2) composites

It was determined that the hardness of fabricated composites increased as the filler content increased, and the S4 composite attained a higher value (51.04 HV) (Fig. 4). This improvement in hardness may be achieved due to the better dispersion of silicon dioxide filler in AF composites. Moreover, silicon dioxide filler can provide resistance against indentation due to its better surface hardness and is collected at the top surface of fabricated composites. Similarly, the optimal conditions were 10 % silane treatment for 20 min with 5 % nano-SiO_2 filler, yielding 26 % and 28 % improvements in flexural strength and hardness, respectively (Arunachalam *et al*. 2025).

Polymer composites often fail in industrial applications where they face impact loading. Therefore, investigation of material damage due to impact is essential for the study of the overall behavior of composites. For this reason, the Charpy impact test was conducted. It was revealed that the S1 composite exhibited low impact energy (3.841 J) due to the AF fibres being predicted to attain a brittle and rigid nature, which reduced the capability of absorbing more impact energy (IE). Conversely, the impact energy of the manufactured composites is likely to be higher due to the evenly distributed silicon dioxide filler in the epoxy matrix (Fig. 6).

The higher value of impact energy is achieved by the S3 (4.225 J) composite, which is 21.40 % higher than the S1 composite. Likewise, the hybrid epoxy composites with jute-palmyra fibers and 0–4 wt % functionalized nano-SiO_2 were evaluated. The 2 wt % SiO_2 variant achieved maximum tensile strength (55.52 MPa), impact strength (4.02 J), and wear resistance, while 3 wt % provided the best flexural strength. These enhancements highlight the viability of SiO_2-based green composites in tribological and structural roles (Nag *et al*. 2024).

Table 2. Design of experiments

S. No.	Sliding Velocity (ms^{-1})	SiO_2 Content (wt %)	Normal Load (N)	SWR (mm^3/Nm) × 10-8	S/N Ratio
1	2	0	20	3.50	-10.8814
2	2	3	25	7.34	-17.3139
3	2	5	30	8.89	-18.9780
4	2	7	35	11.07	-20.8830
5	3	0	25	5.13	-14.2023
6	3	3	20	4.22	-12.5062
7	3	5	35	10.30	-20.2567
8	3	7	30	10.23	-20.1975
9	4	0	30	6.26	-15.9315
10	4	3	35	8.36	-18.4441
11	4	5	20	6.87	-16.7391
12	4	7	25	8.56	-18.6495
13	5	0	35	6.96	-16.8522
14	5	3	30	7.50	-17.5012
15	5	5	25	8.06	-18.1267
16	5	7	20	6.92	-16.8021

3.2. Sliding Wear Performance by Taguchi Analysis

Under arid conditions, the SWR of composites was investigated about control factors. Equation 1 was employed to determine the SWR for each of the 16 test sessions, as illustrated in Table 2 and Fig. 7.

The main effect plot indicates that if the line is nearly horizontal for a parameter, it has little effect on the output response. In contrast, a highly inclined line gives the highest impact of the parameter on the response (Prabhu *et al*. 2024). The main effect plot for the selected control factors affecting the SWR of silicon dioxide nanofiller-based AF composites is shown in Fig. 8.

Additionally, the temperature of the friction surface may be elevated as a result of an increase in sliding velocity, which could potentially have a detrimental effect on the mechanical characteristics. Therefore, the SWR of composites rises as the sliding velocity increases for a given load and material state. The protection of the composite surface, a rise in hardness, and a decrease in the brittleness of the composites are the reasons for the reduction of the WR of composites with the addition of silicon dioxide nano-fillers. Nevertheless, the initial formation of the transfer film is accompanied by a decline in the load from 20 N to 25 N. In order to compact the transfer films, an additional decrease in the load to 30 N may be considered. This reduction in specific wear rate is attributed to the cohesive and compressed tribofilms, while a slight increase in wear rate is observed for further improvement in normal load (35 N). Each control factor plays a distinct role in influencing the SWR of the composites. Silicon dioxide content directly affects the surface hardness and structural integrity of the composite. At optimal loading (5–7 wt %), SiO_2 enhances surface resistance to abrasion by acting as a micro-reinforcement, forming a denser and harder contact surface, which reduces material removal

during sliding. However, excessive filler (beyond 5 wt %) can cause agglomeration, leading to localized weakness and increased wear. Normal load impacts the contact pressure at the sliding interface. Higher loads increase the interaction between the composite and the counterface, promoting better compaction of wear debris and transfer film formation. This can protect the surface at moderate loads (up to 30 N), but excessive load (e.g., 35 N) may exceed the material's stress tolerance, causing microcracks and accelerated wear. Sliding velocity influences the frictional heat generated at the interface. At lower velocities, the temperature rise is minimal, promoting stable wear conditions. As velocity increases, heat buildup can soften the matrix, reduce interfacial bonding, and lead to thermal degradation, increasing wear. In practical applications, such as automotive or structural components, balancing these parameters is crucial to ensure long-term surface durability under varying operational stresses.

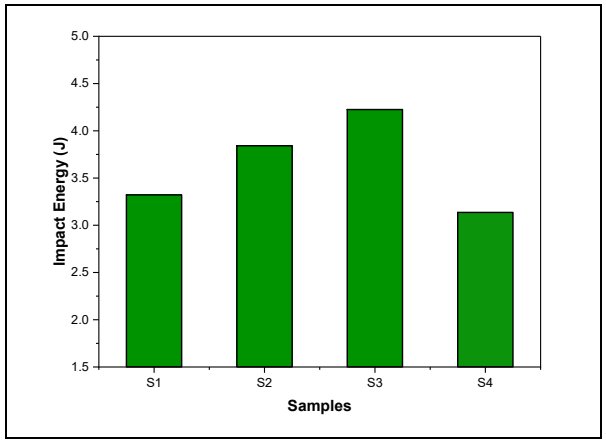


Fig. 6: Influence of SiO_2 content on impact energy of fabricated composites

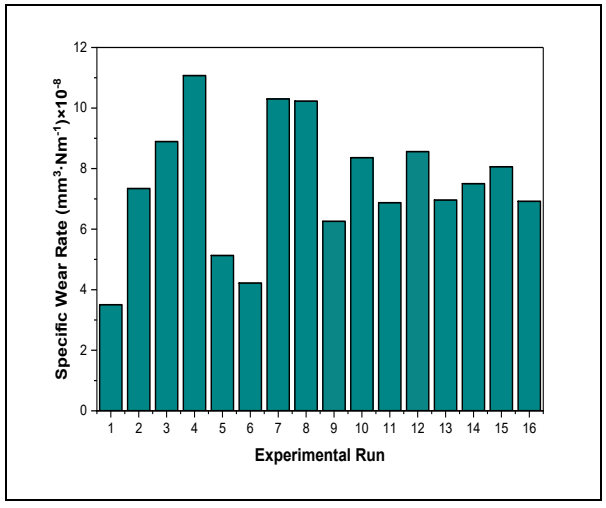


Fig. 7: Evaluation of composite experimental run with respect to specific wear rate

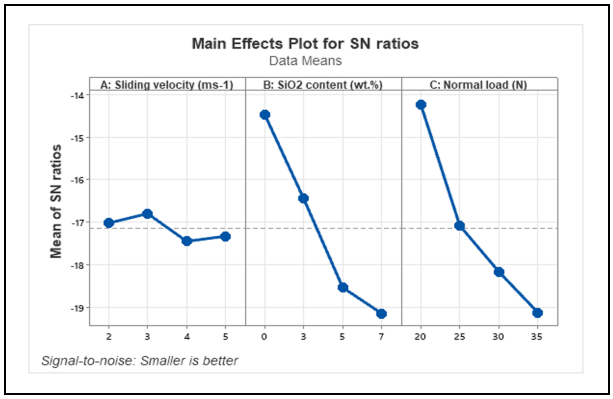


Fig. 8: Influence of control factor on SWR of composites

Table 3. Results on response table for S/N ratios for composites

Level	A (m/s)	B (wt %)	C (N)
1	-17.01	-14.47	-14.23
2	-16.79	-16.44	-17.07
3	-17.44	-18.53	-18.15
4	-17.32	-19.13	-19.11
Delta	0.65	4.67	4.88
Rank	3	2	1

Table 3 shows the response table for the S/N ratio analysis. From the analysis, it is evident that factor A is the most significant factor prompting the SWR resistance, followed by the SiO_2 content. The SWR is least affected by the normal load, and the selected parameters may be ranked in the following order: Sliding velocity (5 ms^{-1}) > SiO_2 content (7 wt %) > normal load (35 N). Additionally, Equation 6 is employed to determine the impact of each control factor on the SWR. The findings indicate that the wear rate of AF composites based on SiO_2 nanofillers is most significantly influenced by the sliding velocity, with a contribution ratio of 60.7 % for SiO_2 content, 46.9 % for the normal load, and 0.40 % for the sliding velocity.

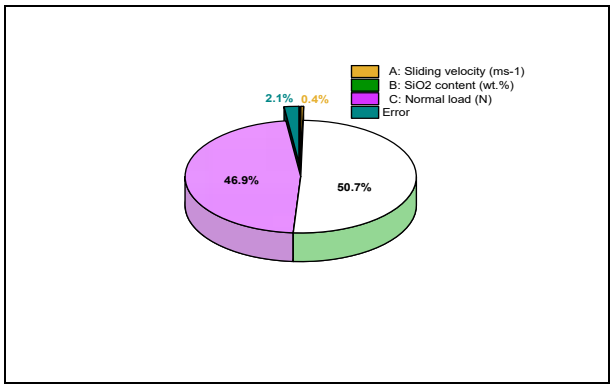


Fig. 9: Contribution of the control parameters on SWR of composites

4. CONCLUSION

The mechanical and wear behavior of *Agave fourcroydes* epoxy hybrid composites reinforced with silicon dioxide nanofillers was systematically investigated. Mechanical properties, including tensile strength, flexural strength, and impact energy, improved with increasing nanofiller content up to 5 wt % due to enhanced interfacial adhesion and uniform dispersion. At 7 wt %, property degradation occurred because of agglomeration, except for hardness. The SEM analysis confirmed reduced fibre pull out and better dispersion at 5 wt %. Wear analysis revealed that normal load and nanofiller content were the most influential parameters. The enhanced performance indicates suitability for lightweight, durable, and sustainable automotive and interior applications.

FUNDING

This research received no specific grant from any funding agency in the public, commercial, or not-for-profit sectors.

CONFLICTS OF INTEREST

The authors declare that there is no conflict of interest.

COPYRIGHT

This article is an open-access article distributed under the terms and conditions of the Creative Commons Attribution (CC BY) license (http://creativecommons.org/licenses/by/4.0/).

REFERENCES

Agaliotis, E. M., Concha, A. B. D., Pat, M. A., Morales, A. J. P., Bernal, C., Valadez, G. A., Herrera, F. P. J., Proust, G., Koh, D J. F., Carrillo, J. G. and Flores, J. E. A., Tensile Behavior of 3D Printed Polylactic Acid (PLA) Based Composites Reinforced with Natural Fiber, *Polym*., 14(19), 3976 (2022). https://doi.org/10.3390/polym14193976

Albert, F. A., Jafrey, D. J. D., Karthik, P. G., John, I. W., Hariharan, S., Guna, A., Haribaskar, L., Sathish, K. G. and Mohanraj, C., Tribological Studies and Optimization of Two-Body Abrasive Wear of NaOH-Treated Vachellia Farnesiana Fiber by Additive Ratio Assessment Method, *J. Mater. Eng. Perform.,* 32(1), 82–90 (2023). https://doi.org/10.1007/s11665-022-07082-y

Anaya, R. R. C., Rios, S. C. R. and Herrera, F. P. J., Identification of micro-failure processes of HDPE-henequen fiber composite material by using acoustic emission monitoring: Effect of fiber surface modification, *Polym. Compos*., 44(5), 2697–2709 (2023). https://doi.org/10.1002/pc.27271

Arumugam, K. and Kaliannagounder, M., Investigation on the mechanical and moisture uptake properties of epoxy-Terminalia arjuna fiber natural composites containing nano-silica, *Int. Polym. Process*., 39(3), 357–366 (2024). https://doi.org/10.1515/ipp-2023-4482

Arunachalam, S. J., Saravanan, R. and Sathish, T., Deep analysis of chemically treated Jute/Kenaf and glass fiber reinforced with SiO_2 nanoparticles by utilizing RSM optimization., *Results Eng*., 26(1), 104523 (2025). https://doi.org/10.1016/j.rineng.2025.104523

Devendrappa, S. K., Sanjeevamurthy, Goud, M., Ravikumar, P. and Naik, V. K. H. S., A Study on Mechanical and Wear Behaviour of Graphite Filled Sisal-Glass-Epoxy Hybrid Composites, *Compos. Theory Pract*., 2022(2), 106–113 (2022).

Erkliğ, A., Bozkurt, Ö. Y. and Al-tekreetı, W. F., Influence of Nano-Silica on the Mechanical Properties of Jute/Glass Fiber Reinforced Epoxy Hybrid Composites, *Cukurova University Journal of the Faculty of Engineering*, 37(2), 399–410 (2022). https://doi.org/10.21605/cukurovaumfd.1146108

Espinach, F. X., Julian, F., Alcalà, M., Vilaseca, F., Carrasco, F. and Mutjé, P., Effective Tensile Strength Estimation of Natural Fibers through Micromechanical Models: The Case of Henequen Fiber Reinforced-PP Composites, *Polym*., 14(22), 4890 (2022). https://doi.org/10.3390/polym14224890

Gavidia, M. P. P. and Salas, A. R. T., Natural fiber reinforced composites (Coconut/Jute/Henequen Fibers) used in the construction of a high-power experimental rocket, *Proc. Int. Astronaut. Congr*. (IAC), 230–238 (2024). https://doi.org/10.52202/078379-0018

Gupta, R. K., Mayakannan, S., Vijayaraghavalu, S., Poornima, M. M., Nanthakumar, S. and Bhaskaran, N. A., Multi-objective Optimization of Bamboo-madar Fiber Reinforced Composites for Lightweight Automotive Applications using Machine Learning and Genetic Algorithms, *J. Environ. Nanotechnol.,* 13(4), 358–376 (2024). https://doi.org/10.13074/jent.2024.12.244978

Gurukarthik, B. B., Prince, W. D., Aravind, B. P. V., Baskaran, R. and Narayanasamy, P., Exploration of Electrical, Thermal, and Mechanical Properties of Phaseolus vulgaris Fiber/Unsaturated Polyester Resin Composite Filled with Nano–SiO_2, *J. Nat. Fibers*, 18(12), 2156–2172 (2020). https://doi.org/10.1080/15440478.2020.1724231

Harak, S. S., Krishnaveni, K., Karthick, K., Chinnarasu, K., Venkata, H. P. P., Tonk, A. and Mayakannan, S., Experimental Study on the Mechanical Properties of Hybrid Areca and Abaca Fiber Reinforced Polymer Composites, *J. Environ. Nanotechnol.,* 13(4), 92–101 (2024). https://doi.org/10.13074/jent.2024.12.244977

Iyyadurai, J., Arockiasamy, F. S., Manickam, T. S., Suyambulingam, I., Siengchin, S., Appadurai, M. and Raj, E. F. I., Revolutionizing Polymer Composites: Boosting Mechanical Strength, Thermal Stability, Water Resistance, and Sound Absorption of Cissus Quadrangularis Stem Fibers with Nano Silica, *Silicon*, 15, 6407–6419 (2023). https://doi.org/10.1007/s12633-023-02510-7

Jagadeesh, P., Puttegowda, M., Suyambulingam, I., Gupta, M. K., Mavinkere, R. S. and Siengchin, S., Analysis of friction and wear performance of eco-friendly basalt filler reinforced polylactic acid composite using the Taguchi approach, *J. Thermoplast. Compos. Mater*., 37(7), 2479–2504 (2023). https://doi.org/10.1177/08927057231211231

Kedarnath, M. P., Ramasamy, N., Anand, M. D. and Raj, J. B., Exposing the role of silica nanoparticles and fiber stacking in mechanical, water absorption, and bio-degradation behaviors of banana-papaya hybrid composites, *Phys. Scr*., 100(1), 015034 (2025). https://doi.org/10.1088/1402-4896/ad9cd0

Kim, J. and Cho, D., Effects of Alkali-Treatment and Feeding Route of Henequen Fiber on the Heat Deflection Temperature, Mechanical, and Impact Properties of Novel Henequen Fiber/Polyamide 6 Composites, *J. Compos. Sci.,* 6(3), 89 (2022). https://doi.org/10.3390/jcs6030089

Kumar, R., Ganguly, A., & Purohit, R., Optimization of mechanical properties of bamboo fiber reinforced epoxy hybrid nano composites by response surface methodology, *Int. J. Interact. Des. Manuf*., 18(9), 6479–6492 (2024). https://doi.org/10.1007/s12008-023-01215-w

Lakshmaiya, N., Chukka, N. D. K. R., Kaliappan, S., Balaji, V., Ross, N. S. and Maranan, R., An integrated Artificial neural network technique to optimize the various parameters of Pineapple/SiO_2/epoxy-based nanocomposites under NaOH treatment, *Results Eng*., 26, 104737 (2025). https://doi.org/10.1016/j.rineng.2025.104737

Mary, G. A. A., Uma, P., Ramya, R., Sunitha, T. and Devi, R., Characterization of Mechanical Properties of Ramie/SiO_2 Hybrid Composite by Incorporation of Kenaf Fiber, *J. Environ. Nanotechnol.,* 13(3), 449–455 (2024). https://doi.org/10.13074/jent.2024.09.242767

Mathur, N. M., Yashpal and Pratap, B., Ascertaining Tribological Properties of PLA Matrix Composites Reinforced with SCB/CF Fiber with ANOVA and Regression Analysis, *Evergreen*, 11(1), 234–241 (2024). https://doi.org/10.5109/7172260

Nag, M. K. and Kumar, P., Design, development and effect evaluation of silica nanoparticles on the physical, mechanical, and tribological behaviour of jute/palmyra fiber-reinforced hybrid nanocomposites, *J. Mech. Sci. Technol.,* 38(11), 6075–6084 (2024). https://doi.org/10.1007/s12206-024-1025-9

Narayanan, L. and Muthukumaran, S., Development of silane-treated corn husk fiber and agro-waste biofiller-reinforced epoxy composite: effects on wear, mechanical, thermal, and water absorption properties, *Biomass Convers. Biorefin.,* 14(23), 30801–30817 (2024). https://doi.org/10.1007/s13399-024-05837-2

Padma, R. A., Vemula, A. M., Prakash, B. M., Kumar, P. S., Murali, K. V. and Janaki R. P., Effect of Ceramic Nano Fillers in Jute Fibre Composites, *Adv. Mater. Sci. Eng*., 2022(1), 3057829 (2022). https://doi.org/10.1155/2022/3057829

Prabhu, R., Mendonca, S., Bellairu, P. K., D'Souza, R. and Bhat, T., Modeling and analysis of TiO2 filler's impact on specific wear rate in flax fiber-reinforced epoxy composite under abrasive wear using Taguchi approach, *Multidiscip. Model. Mater. Struct.,* 20(3), 546–557 (2024). https://doi.org/10.1108/MMMS-10-2023-0342

Raja, T., Exploring a natural fiber extracted from henequen plant leaves: A sustainable innovation for reinforcement in composite materials, *Results Eng*., 25, 104015 (2025). https://doi.org/10.1016/j.rineng.2025.104015

Rosas, D. F., García, H. D. G. and Juárez, A. C. A., Development of Lignocellulosic-Based Insulation Materials from *Agave fourcroydes* and Washingtonia filifera for Use in Sustainable Buildings, *Sustainability (Switzerland),* 16(13), 5455 (2024). https://doi.org/10.3390/su16135455

Rout, I., Singh, M., Mahapatra, T. R., Mishra, P., Dash, S. and Mishra, D., Characterization and Optimization of Dry Sliding Wear Properties of Partially Biodegradable Hybrid Polymer Composites, *J. Bio-Tribo-Corros*., 11(2), 59 (2025). https://doi.org/10.1007/s40735-025-00979-w

Salinas, B. M. J., Torres, G. M. T., Paniagua, M. M., Sánchez, M. M. and Cabello, J., Clonal mechanisms that matter in *Agave fourcroydes* and A. sisalana invasions in drylands: implications for their management, *Manage. Biol. Invasions*., 14(1), 80–97 (2023). https://doi.org/10.3391/mbi.2023.14.1.04

Sarkar, D., Borah, P., Samanta, S., Teyi, N., Chetia, P. and Borah, R., Tribo-performance of saw dust filled natural fiber – Glass fiber reinforced epoxy composites: Modelling and optimization, *Mater. Today Proc*., 80(2), 904–910 (2023). https://doi.org/10.1016/j.matpr.2022.11.326

Seeniappan, K. and Natrayan, L., Surface Modification of Henequen Fibers with Catalyst for Improving Mechanical and Thermal Properties in Phenolic Composites for Automotive Uses, *SAE Tech. Pap*., 1, 5029(2024). https://doi.org/10.4271/2024-01-5029

Serra, P. F., Vilaseca, F., Aguado, R., Espinach, F. X., Tarrés, Q. and Delgado, A. M., Effective young's modulus estimation of natural fibers through micromechanical models: The case of henequen fibers reinforced-pp composites, *Polym.,* 13(22), 3947 (2021). https://doi.org/10.3390/polym13223947

Venkatesha, P. G., Nikhil, M. and Sai, K. A., Effect of Hybridization, Influence of Surface Modification on the Properties and Optimization of bio fiber Composites, *Lect. Notes Mech. Eng*., 26, 209–218 (2020). https://doi.org/10.1007/978-981-15-7557-0_19

Vignesh, S., Bensam, R. J., Viswanath, K. and Natarajan, N., Experimental investigation on the behavior of epoxy/peepal composites fortified with silica and silicon carbide nanoparticles for industrial applications, *Wood Mater. Sci. Eng*., 19(3), 718–724 (2024). https://doi.org/10.1080/17480272.2023.2289033

Zeng, S. H., Wei, C., Zeng, M., Xiong, X. M., Liu, H. X., Lv, J. and Qin, A. M., Friction properties of sisal fiber reinforced nano-SiO_2 phenol formaldehyde resin brake composites, *Appl. Mech. Mater.,* 490, 64–68 (2014). https://doi.org/10.21605/cukurovaumfd.1146108